An Efficient Electrochemical Sensor Based on Zirconium Molybdate Decorated Reduced Graphene Oxide for the Detection of Hydroquinone

Nandini Nataraj[1], Tse-Wei Chen[2], Shen-Ming Chen[1,], Syang-Peng Rwei[3,4]*

[1] Department of Chemical Engineering and Biotechnology, National Taipei University of Technology, No.1, Section 3, Chung-Hsiao East Road, Taipei 106, Taiwan.
[2] Department of Materials, Imperial College London, London, SW7 2AZ, United Kingdom
[3] Research and Development Center for Smart Textile Technology, National Taipei University of Technology, Taiwan
[4] Institute of Organic and Polymeric Materials, National Taipei University of Technology, Taiwan
[*]E-mail: smchen78@ms15.hinet.net, smchen1957@gmail.com

The present work concentrates over the electrochemical sensing of hydroquinone (HQ) with modified Zirconium Molybdate Decorated Reduced Graphene Oxide ($Zr(MoO_4)_2$ @rGO/GCE). $Zr(MoO_4)_2$@rGO was synthesized by a facile hydrothermal method. Followed with the characterization of the as prepared material was examined with XRD, FTIR and FESEM along with their application was employed with cyclic voltammetry technique. Results obtained from XRD and FTIR clearly demonstrated that $Zr(MoO_4)_2$@rGO have been formed with good crystallinity and morphology. Differential pulsed voltammetry studies further declared the limit of detection and Linear range as 0.015 μM and 0.01-250 μM with the sensitivity about 0.02042 μA μM^{-1} cm^{-2}. River water, waste water and tap water were implied for the real time applicability of the fabricated sensor. Interference studies as performed revealed that no other similar compounds have been interfered with HQ and along with this the repeatability, reproducibility and stability performances explains the excellent behavior of the as prepared sensors efficiency in repeated cycles and in numerous electrodes. Thus, the fabricated sensor could be a simple, effective and selective sensor for detection of HQ.
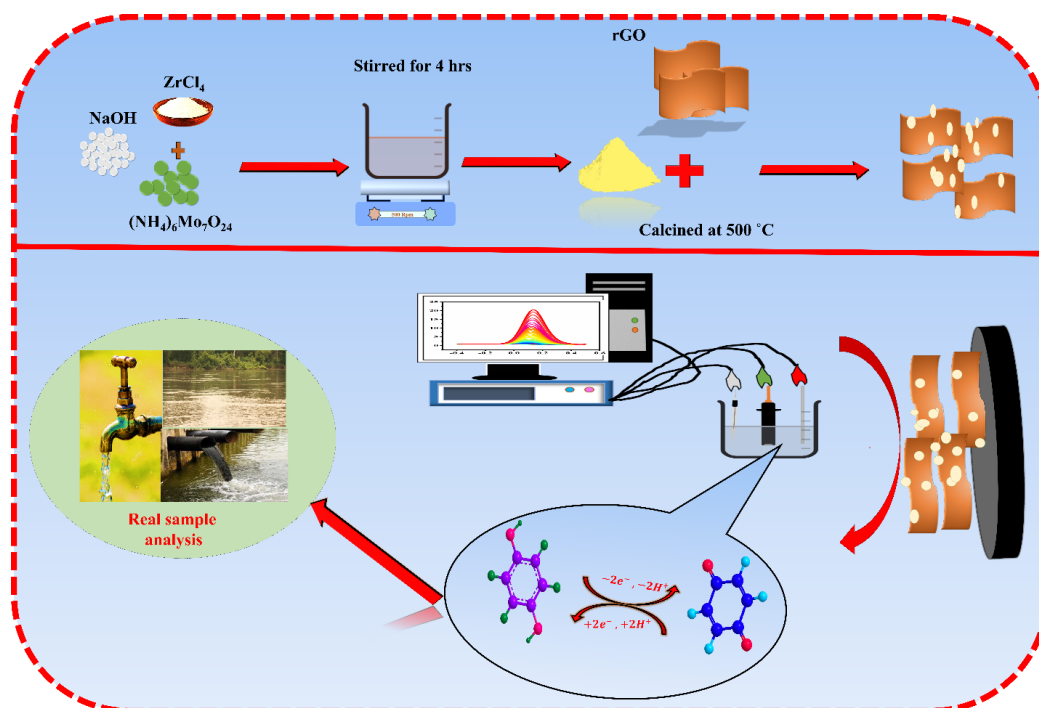
1. INTRODUCTION

We exist in a vast world with several organic and inorganic products being employed by all the peoples majorly produced by the chemical industries as in the branches of cosmetics, pesticides,

fungicides, food beverages, food products, hair dyes, oil refinery etc., [1], [2] Coming under this topic several waste products or the by-products are being left over which correlates the major threat, affecting life with several causes for both human and wild life including aquatic life with drastic influences. Among this comes the aromatic compounds being one among them, as several groups described and distinguished the hydroquinone (HQ) are harmful with its exposure and followed with its effective reactions are targeted in this report [3]. HQ is one type of phenols which are being employed in the field of textiles, plasticizers, cosmetics and pharmaceutical industries [4], [5]. Majorly it is recognized in cosmetic products as a therapy of curing the pigmentation of melanin (causing brown pigment) in skin, melasma, chloasma, skin whitening- as creams, age spots [6]. Although being used in several applications it is regarded as an environmental pollutant due to its left over after production which remains in the land causing tremendous effects. This happens as they hold low biocompatible nature and toxic behavior [7]. Chemically called as 1, 4, -dihydroxy benzene is considered to be the isomers of dihydroxybenzene and synchronizes with other compounds as catechol and resorcinol with their parallel properties [8]. They have the ability of being carcinogenic, haematotoxic and genotoxic with non-degradable risk and with multiple health issues are also noticed with its consumption [9]. Some of the problems being linked to human beings are leukemia, skin irritation, vascular collapses, DNA damage, pulmonary failure, tachycardia etc., [10], [11]. Several methods are being used for the detection of this particular compound with huge collections of data. But, being lagged with unsatisfied properties as like high cost, tedious job with the handling procedure, time consuming made techniques like liquid chromatography, chemi-luminescence technique, flow injection analysis are with less considerable [12], [13], [14]. Here come the electrochemical methods offering all the desired properties as sufficient time saving, affordable, easy procedure and as such. Electrochemical methods are an excellent substitute offering very low sensitivity, fouling of signals, providing a platform for low detection limits etc.,

Exploring out in the field of materials in a varied way and exposing it towards several applications are sort out attention in trending research. As in that case the material with several desired properties with lots of performances are to be recognized. Coming under the class of transition metals zirconium and molybdate with their dual performance are opted for their amazing properties. As zirconium-based materials holds tremendous properties as good ionic conductivity, chemical and thermal stability, high fracture toughness, corrosion and microbial resistive tolerance, very less thermal conductivity [15], [16]. With a fine natural color, it is finely used up in different fields in sensors, fuel cells, supercapacitors, in electronics, medical related ways and also in magnetism-based applications etc., like thermal barrier coatings, as catalyst support, a core material as such [17], [18]. Looking interior they have large vacancies of oxygen on their surface and with opting techniques to be employed for further interactions with other materials for usage in other fields [19], [20]. And molybdenum are also effective with several properties as like zirconium with good electroactive ability, thermal stability etc., utilized in variety of applications [21]. Zirconium molybdates are trending with variety of applications as being a catalyst support, is mainly concentrated due to their ion exchange capability, and redox movement and this ability makes them used up as refractory material and thermal barrier coating [22]. It is also utilized as transistors as an insulator and their crystal morphology are assigned to be tetragonal, cubic and monoclinic. They can be prepared by a huge number of methods as like chemical and physical methods, co-precipitation method, sol gel, hydrothermal method, chemical reflux method etc., Herein,

hydrothermal method was performed keeping the most advantageous implications like obtaining good morphology, low agglomeration of nanoparticles, great purity, even composition, phase homogeneity etc., Although $Zr(MoO_4)_2$ has good electro-catalytic activity when desired to modify with carbon material brings out good outbreak in recent work. Under carbon based materials several are optional whereas multi-walled carbon nanotubes, graphene oxide, carbon nanofibers, reduced graphene oxide etc., Obviously, reduced graphene oxide which is a two dimensional material with sp^2 bonded carbon atoms offers a wide field of applications for various metals/metal oxides/metal sulfides [23]. It holds a hydrophobic nature with vander-waals interaction and strong π-π stacking providing good electrical and thermal property [24]. This ideal material shows excellent sensing ability towards hydroquinone (HQ).

Several researchers have discovered zirconium based and rGO based materials and also molybdenum as their selective material for several applications as like Manthrapudi Venu *et al.,* has synthesized zirconia nanoparticle decorated reduced graphene oxide for the detection of anticancer drug regorafenib [25], Sivaprakasam radhakrishnan *et al.,* have synthesized polyaniline nanofiber incorporated iron oxide with reduced graphene oxide for the detection of hydroquinone [26], Apinya puangjan *et al.,* have worked on zirconium oxide-cobalt oxide supported reduced graphene oxide for simultaneous detection of gallic acid, caffeic acid and protocatechuic acid but zirconium molybdate anchored reduced graphene oxide for the detection of hydroquinone (HQ) has not been reported as per our survey of literature. In case of electrochemical method has been chosen due respect with their significances as cost effective, high accuracy, fast reactive property, simple method, easily handled made its utilization in huge rate. Hence, this report concerns the work as $Zr(MoO_4)_2$/rGO for HQ detection and further its physical and chemical characters were determined by XRD, FTIR, and cyclic voltammetry technique for application purposes.

Scheme 1. Schematic description of synthesis and electrochemical sensing application of $Zr(MoO_4)_2$/rGO.

2. MATERIALS AND INSTRUMENTATION UTILIZED

Zirconium chloride [$ZrCl_2$], ammonium heptamolybdate [$(NH_4)_6Mo_7O_{24}$] and urea [CH_4N_2O] was utilized for the synthesis of zirconium molybdate. Distilled water (DI) was employed all over the experimental process for both synthesis and washing purposes along with ethanol was also further utilized. Lake water collected form new Taipei city lake and for waste water it was taken from Taipei city sewage and for tap water collected from Taipei locality which were all used for real sample analysis. Other samples like hydroquinone (HQ), ascorbic acid (AA), glucose (Gu), potassium ions (K^+), sodium ions (Na^+), potassium bromide (KBr), sodium nitrate ($NaNO_2$), uric acid (UA) was employed for interference studies obtained from Sigma Aldrich, Taiwan.

For the analysis of structural characters XPERT PRO X-ray diffraction (XRD) were used, Fourier transform infra-red spectroscopy - Perkin-Elmer IR spectrometer was employed, Field emission scanning electron microscopy (FE-SEM, A ZEISS sigma 300) and energy-dispersive X-ray spectroscopy (EDX) for the morphology and elemental recognition. Cyclic voltammetry (CV) CHI 750A and differential pulse voltammetry (DPV) CHI 900 electrochemical workstations (CH Instruments Company, made in the U.S.A) were both used for performing electrochemical studies.

2.1. Synthesis procedure

Zirconium molybdate was synthesized by facile hydrothermal method as in the first step 0.05 M of zirconium chloride was dissolved in 50 mL of DI water followed with the addition of 0.1 M ammonium heptamolybdate. After 30 minutes stirring the solution was introduced with urea 0.5 M left undisturbed for one hour under stirring condition. Finally, the solution was transferred into 50 ml Teflon coated autoclave maintained at 180 °C. The obtained solution was centrifuged with DI water and ethanol two times, dried and calcined at 600° C for 3 hours [27]. For the preparation of zirconium molybdate/reduced graphene oxide [$Zr(MoO_4)_2$/rGO] the as prepared $Zr(MoO_4)_2$ was further sonicated with rGO and dried in oven. The as prepared white powder $Zr(MoO_4)_2$/rGO was further used for all the characterization purposes.

2.2. Fabrication of glassy carbon electrode with Zr(MoO₄)₂/rGO

$Zr(MoO_4)_2$/rGO after the confirmation of the elemental presence was taken for electro-chemical studies. In-order, to perform such studies the working electrode was to be fabricated with $Zr(MoO_4)_2$/rGO. The glassy carbon electrode was cleaned with alumina slurry to obtain a clean surface free of other impurities as like mirroring surface at ambient temperature forming a thin film. Along with that the sonicated 3 mg of $Zr(MoO_4)_2$/rGO in 1 mL of DI water was drop casted over the dry electrode surface and used throughout the procedure.

3. RESULT AND DISCUSSION

3.1. XRD and FTIR analysis

Further in order to confirm the structural and crystallinity analysis XRD pattern was recorded. Figure 1a depicts the XRD patterns of rGO, $Zr(MoO_4)_2$ and $Zr(MoO_4)_2$/rGO whereas the composite material $Zr(MoO_4)_2$/rGO agrees with the JCPDS No-00-038-1466 and their respective plane values as (002), (112), (103), (211), (300), (220), (222), (321), (006), (410), (412), (330), (332), (600), (520), (604), (327) are assigned to the theta values 15.85°, 23.35°, 25.75°, 27.25°, 30.55°, 35.35°, 38.95°, 45.85°, 46.45°, 47.65°, 50.05°, 54.25°, 56.65°, 63.55°, 66.85°, 72.55°, and 73.95° respectively. The existence of $Zr(MoO_4)_2$/rGO is very well understood with integration of values with the JCPDS No values as obtained. And the presence of carbon compound used as a core material to improve the property of $Zr(MoO_4)_2$ is being present at theta value 42.55° as it is submerged with the peaks of $Zr(MoO_4)_2$ when taken for the composite material. And also the composite material exhibits a tetragonal structure. Thus from the XRD pattern being obtained shows that the composite material $Zr(MoO_4)_2$/rGO has proved with their presence with good crystallinity.
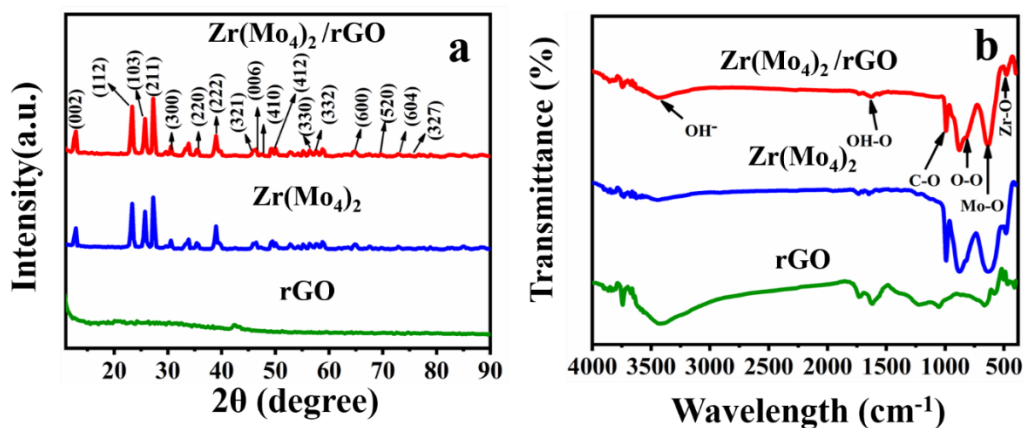

Figure 1. (a) XRD pattern of rGO, $Zr(MoO_4)_2$, and $Zr(MoO_4)_2$/rGO and **(b)** FTIR spectra of rGO, $Zr(MoO_4)_2$, and $Zr(MoO_4)_2$/rGO.

Fourier transform infra-red spectroscopy is employed to fingerprint the recognized elements present in the desired material. Figure 1b represents the FTIR spectrum of $Zr(MoO_4)_2$, rGO and $Zr(MoO_4)_2$/rGO with separate spectral description. For $Zr(MoO_4)_2$ at (b) we could describe the wavelengths at 477 cm^{-1}, 632 cm^{-1}, 874 cm^{-1}, 994 cm^{-1}, 1652 cm^{-1}, 1740 cm^{-1}, 3445 cm^{-1} and for rGO at 1628 cm^{-1}, 1739 cm^{-1}, 3419 cm^{-1}, 1057 cm^{-1}, 658 cm^{-1} and for ZrMo$_4$/rGO IR spectra being araised in combination of both $Zr(MoO_4)_2$ and rGO at different wavelengths. The IR spectra aroused at 3443 cm^{-1} represents the OH group along with 1636 cm^{-1} due respect to the OH-O bond which corresponds to the presence of water molecules formed in accordance with the hydrogen bond formation [28]. The signal at 809 cm^{-1} the O-O stretching along with 881 cm^{-1} the asymmetrical stretching of Mo-O, 635 cm^{-1}

explains the symmetrical stretching of Mo-O and 476 cm^{-1} shows the presence of Zr-O bending vibrations [29]. FTIR analysis have further proved the presence of the material with the spectrum being obtained.
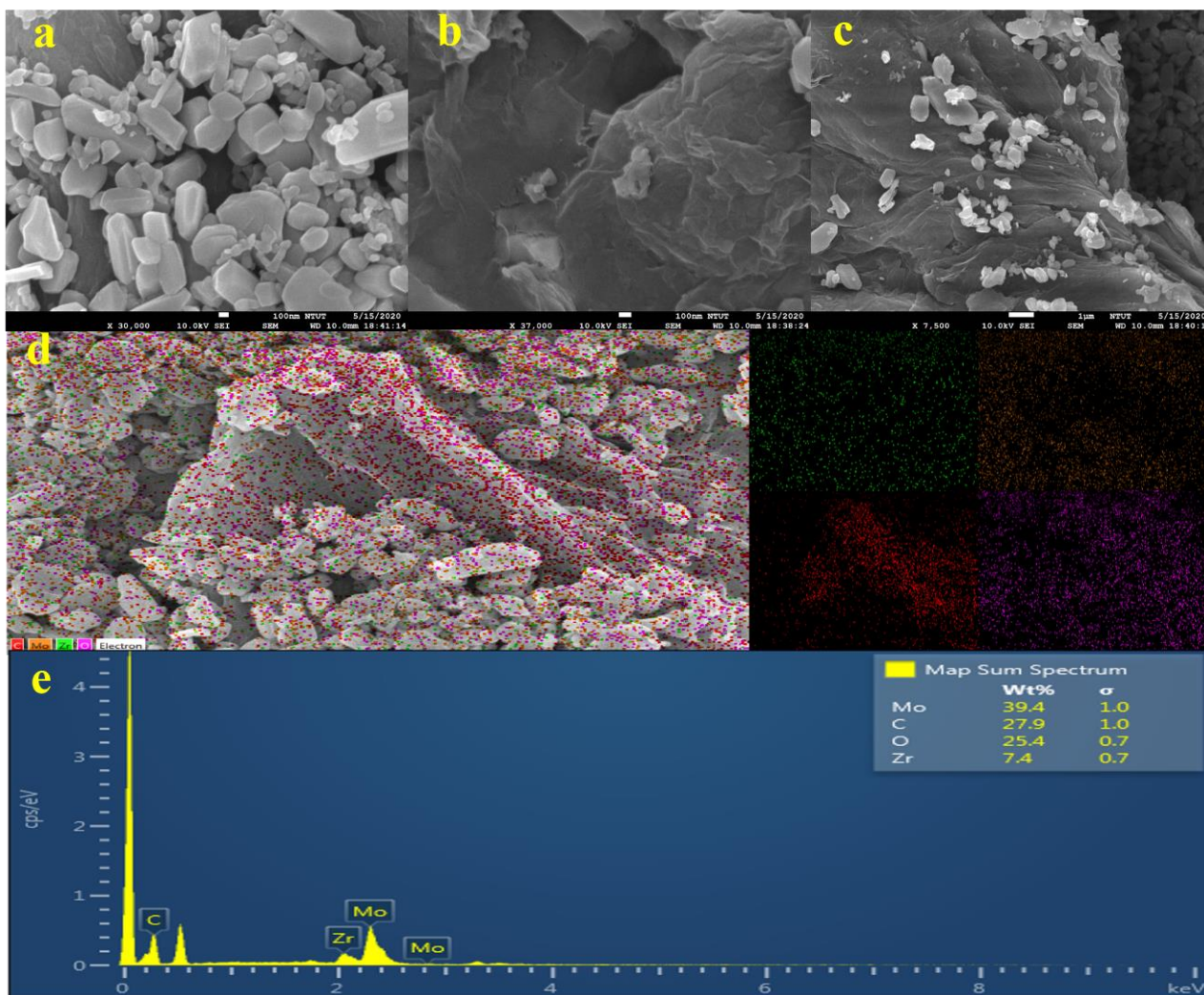

Figure 2. FESEM photographs of (a) ZrMo$_4$ (b) rGO (c) ZrMo$_4$/rGO (d) elemental mapping and (e) EDAX spectrum.

3.2. FESEM analysis

In order to confirm the morphological characters of the material FESEM analysis was done. As Figure 2a represents the formation of Zr(MoO$_4$)$_2$ as like irregular shaped spheres agglomerated at a particular cite. Figure 2b shows the rGO sheets and Figure 2c showing as Zr(MoO$_4$)$_2$ being decorated over the rGO sheets. We could further confirm the presence of ZrMo$_4$/rGO with elemental mapping and EDAX spectrum as shown in Figure 2d illustrating the elemental mapping of ZrMo$_4$/rGO and Figure 2d its EDAX spectrum. Clearly, we could recognize the morphological characters.

3.3. Electrochemical analysis

3.3.1. Electrochemical impedance spectroscopy

Electrochemical impedance spectroscopy is obviously used to investigate the interfacial performance of the desired materials surface with the electrode. Figure 3a shows the electrochemical impedance spectroscopy studies of bare GCE, $Zr(MoO_4)_2$/GCE, rGO/GCE and $Zr(MoO_4)_2$/rGO/GCE. The Rct values as calculated from the EIS spectrum of each material as for bare GCE was about 395.47 Ω for $Zr(MoO_4)_2$ was about 404.69 Ω for rGO almost 159.79 Ω and finally for the composite material $Zr(MoO_4)_2$/rGO was about 75.89 Ω. The Rct values as resembling the resistance values of different modified electrodes and high to low resistance values explains the conductivity of the respective modified electrode. The bare GCE experiences very low conductivity and $Zr(MoO_4)_2$ have little higher conductivity in comparison to bare GCE as the insufficient electron transfer activity. But rGO holding higher conductivity than $Zr(MoO_4)_2$ as 159.79 Ω which can offer better conductivity. Thus the kinetic barrier for the betterment of the transfer of electrons in the electrode is being well established. The change in conductivity attributes to the significant reaction mechanism to be happened and for the detection of HQ in a good manner.

3.3.2. Cyclic voltammetry studies

Cyclic voltammetry studies were done as to well understand the strategies being occurred between the modified electrodes and the analyte. Herein, HQ was desired for the application with $Zr(MoO_4)_2$/rGO modified GCE. This was performed in PB solution as electrolyte with three electrode system at 50 mVs^{-1}. All the modified electrodes were depicted as a comparison with their responses. Figure 3b shows the cyclic voltammograms of $Zr(MoO_4)_2$/GCE, rGO/GCE, $Zr(MoO_4)_2$/rGO/GCE with respective peaks. $Zr(MoO_4)_2$/rGO/GCE exhibits higher redox peaks with the addition of HQ than the other two modified electrodes $Zr(MoO_4)_2$ /GCE and rGO/GCE. The unmodified electrode shows very low current response due to the low electron transfer kinetics between the electrode and the analyte. The enhanced peak response of $Zr(MoO_4)_2$/rGO modified GCE is due to the effective and efficient transfer of electrons between $Zr(MoO_4)_2$/rGO/GCE and HQ. As the Epa is upon positive potential and Epc onside to negative potential indicating the irreversible process of the performed reactions.

$Zr(MoO_4)_2$/rGO/GCE HQ is one of the reactive compound and when analyzed for redox cycles produces reactive oxygen species. After further modifications of the electrode materials pH studies one of the required and important strategy is to be performed. Different pH ranging from 3, 5, 7, 9, 11 were done to optimize the perfect pH range for the detection of HQ. Figure 2c shows the redox peak current of different pH ranges. This was performed within the potential window of -0.4 to 0.6 and with the scan rate of 50 mVs^{-1} and the respective pH as electrolyte solution. With the increase in the pH range the redox peak current shifts more towards the negative potential with their respective currents. The pH range at 7 was recognized to be the opted medium as it experienced more current than the other pH ranges for the detection of HQ. And the lesser current response alongside of acidic medium was assigned to the protonation of HQ. Figure 2d showing the respective linearity plot for pH studies. The linear

equation as calculated was y=0.1479x + 7.4831 for oxidation curve and y=-0.0634x-9.343 for the reduction peak response along with the correlation coefficient was R^2=0.0234 and R^2=0.018 respectively. The redox current as obtained are in response to the involvement of protons during the process. Thus due to the phenolic compounds having the ability to comprise transfer of protons as a result of producing quinoline. The reaction mechanism involved at $Zr(MoO_4)_2$/rGO/GCE for the oxidation of HQ is that hydroquinone reduces to 1,2-benzoquinone with respect to the electrode surface. Figure 5. shows its respective reaction mechanism taken place over the $Zr(MoO_4)_2$/rGO modified glassy carbon electrode. And this in accordance of pH is related as at pH – 7 the current response experienced is more compared to the other pH ranges as the involvement of equal number of electrons and protons as the influence of pH [30][31].
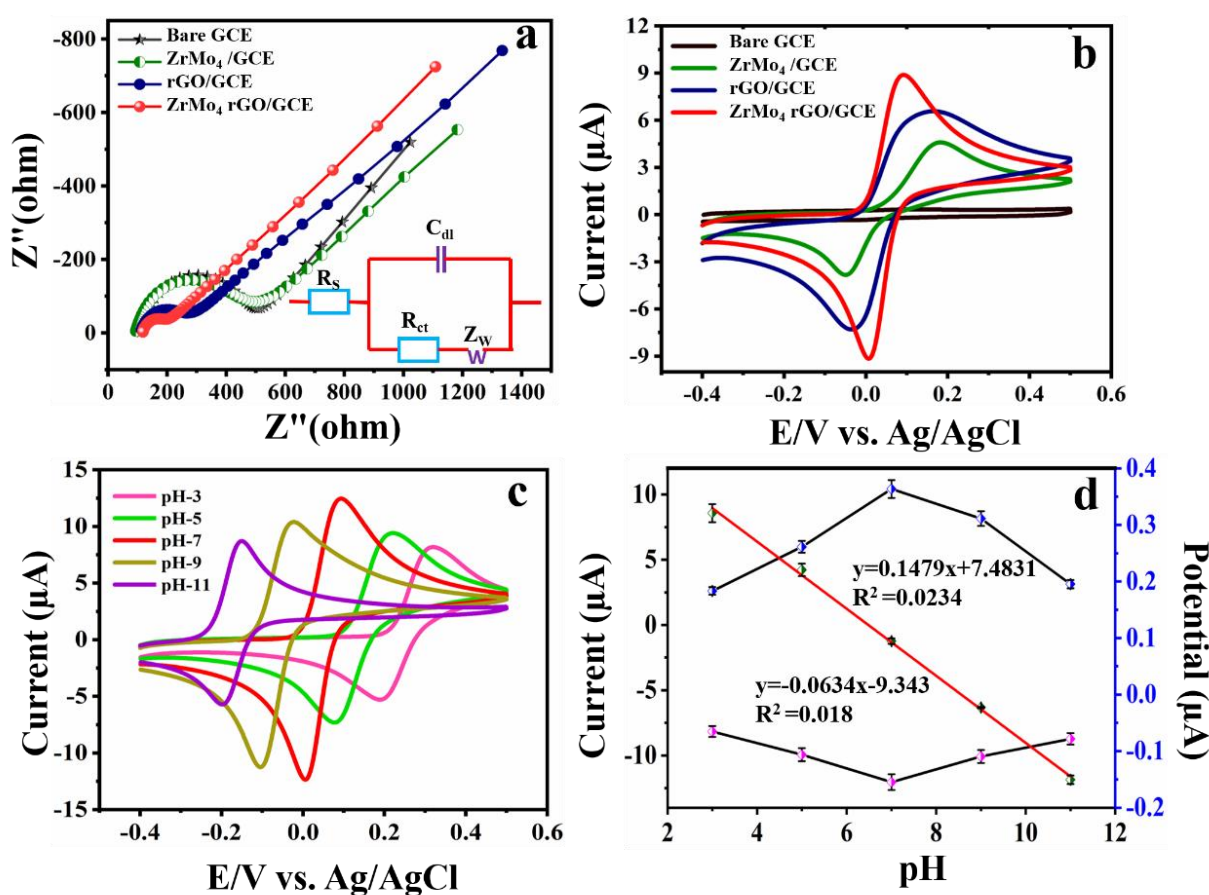

Figure 3. (a) EIS plots of GCE modified $Zr(MoO_4)_2$, rGO and $Zr(MoO_4)_2$/ rGO (b) different film comparison (c) varying pH studies (d) linearity plot of Ph.

On varying the concentrations of HQ ranging from 50 µM to 500 µM redox cycles were recorded as to validate the current response of HQ on different concentrations with the same potential range as performed for pH studies at 50 mVs^{-1} with the GCE modified $Zr(MoO_4)_2$/rGO submerged in phosphate buffer solution. Figure 4a shows the different concentration performance of HQ ranging from 50 µM to 500 µM and their respective linear plots are shown in Figure 4 b for both reduction and oxidation peaks.

As observed from the plot the regression equation was y=0.1291x-1.1743 and y=-0.1404x+1.8334 for both oxidation and reduction peak current responses. In accordance the calculated R^2 values were R^2=0.9941, R^2=0.9918. The increased concentration of the ions as with the increased HQ level is responsible for the increasing current response being the ionic strength of HQ.

Different scan rate performances were obtained as ranging from 20 mVs^{-1} to 200 mVs^{-1}. Figure 4c showing its different scan rate performances from 20 mVs $^{-1}$-200 mVs $^{-1}$. Its corresponding linearity plot is depicted in fig.4d with the linear equation as y=110.72x + 9.002, R^2=0.9905, y=-91.567x-10.189, R^2=0.9908. Concluding that the process underwent a diffusion-controlled process. Since, Zr(MoO$_4$)$_2$/rGO is an p-type semiconductor oxide its major charge carriers will be the holes, whereas, the electrons present in the conduction band with the presence of oxygen it could be reduced to oxidizing species as in their absence no such process occurs. Same as, when introducing HQ it is reduced to benzoquinone thus releasing the electrons with good electro-conductive nature without which it is being lagged [32].
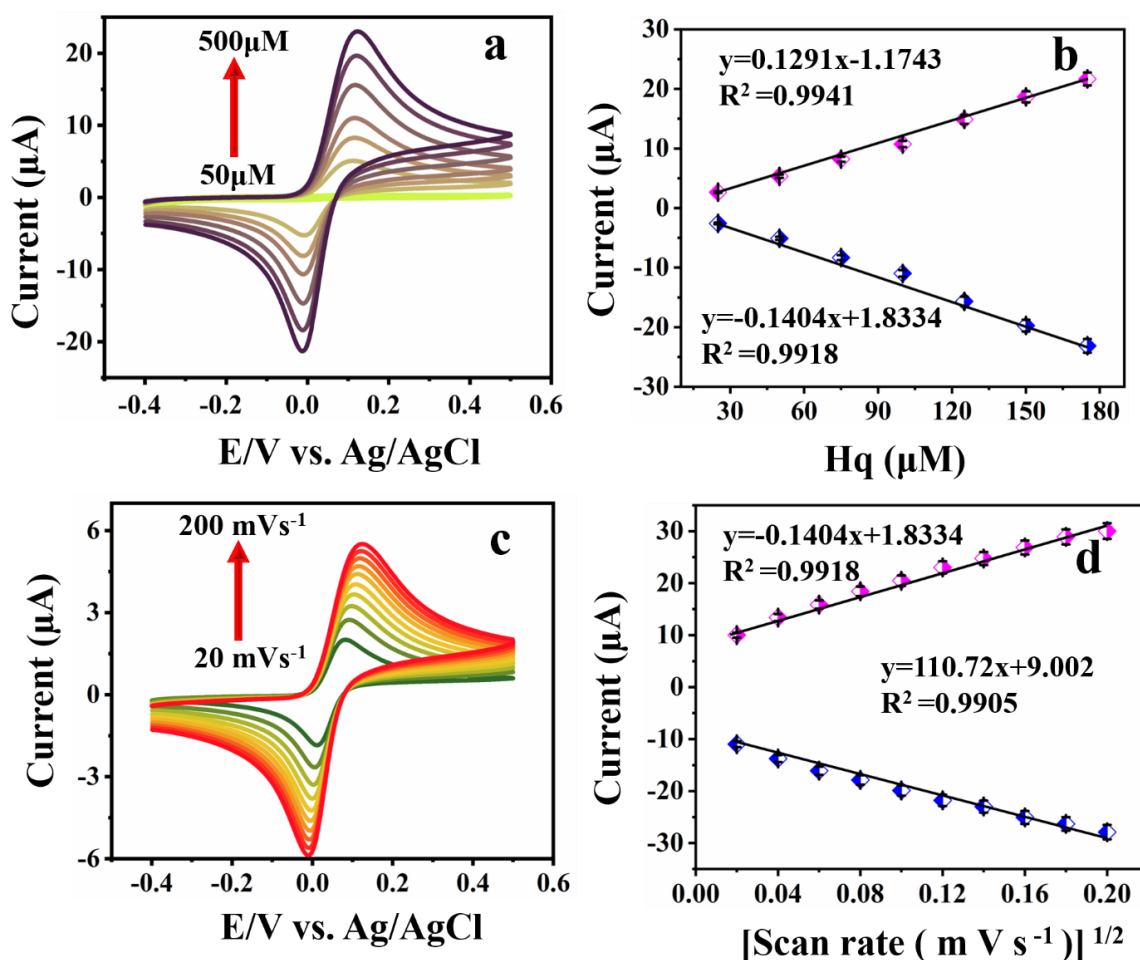

Figure 4. showing the cyclic voltammograms of Zr(MoO$_4$)$_2$/rGO (a) different concentration ranging from 50-500 μM in the presence of 0.1 M of PB solution at 50 mVs^{-1} (b) respective linearity plot of (a). (c) shows the scan rate performed for Zr(MoO$_4$)$_2$/rGO ranging from 20 – 200 mVs^{-1}and (d) linearity plot.
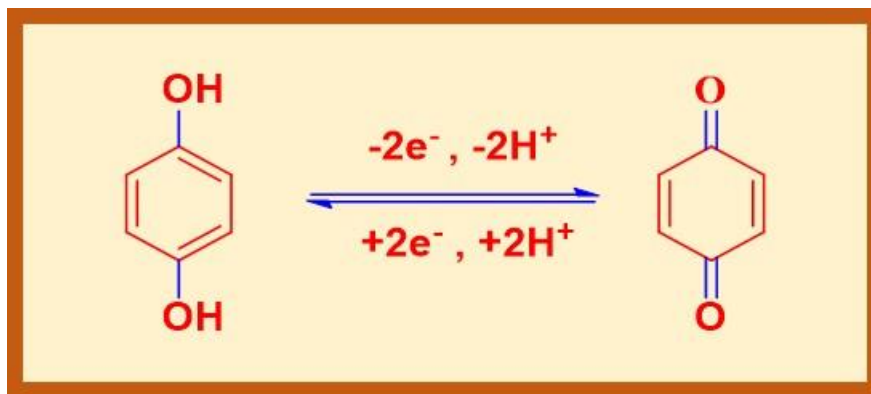
Figure 5. Reaction mechanism of HQ over the Zr(MoO$_4$)$_2$/rGO modified electrode.
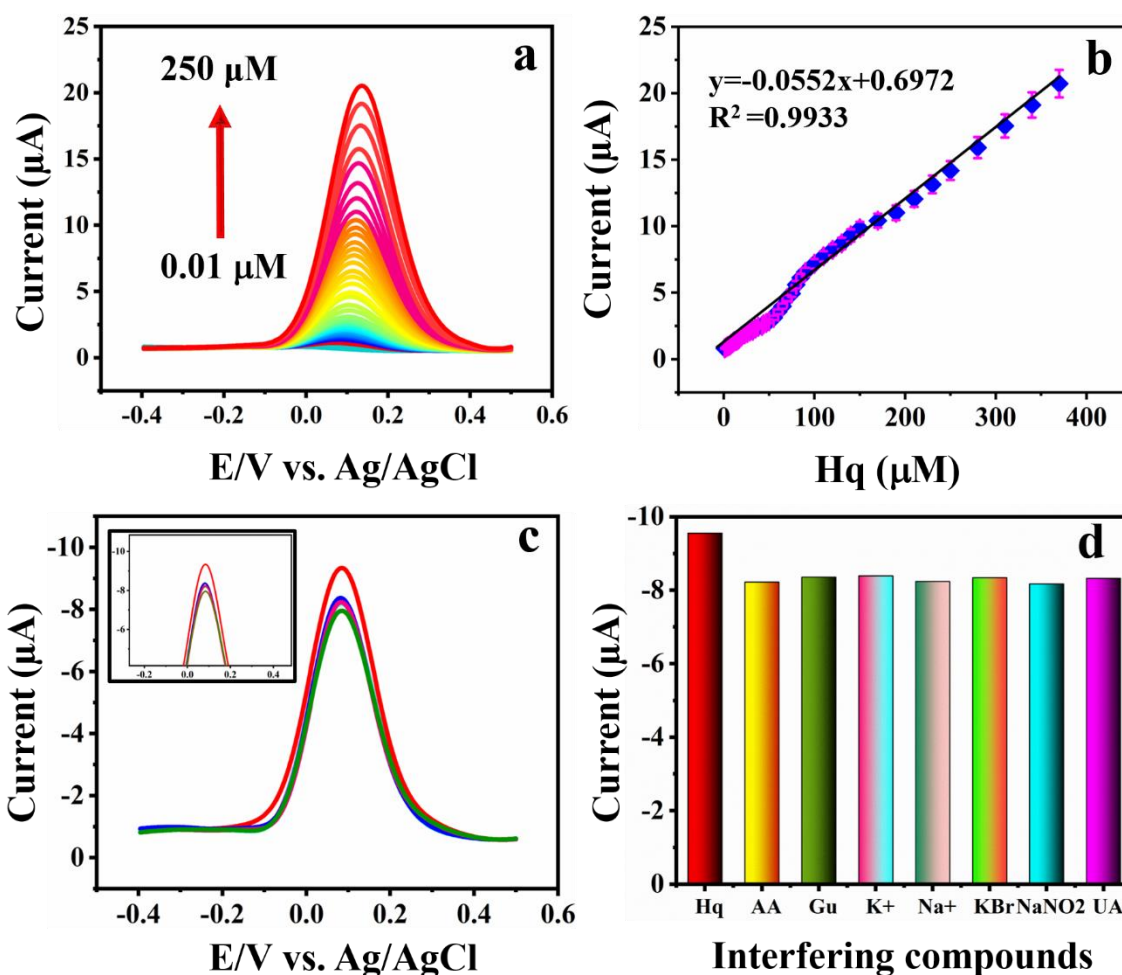
3.3.3. Differential pulsed voltammetry

Figure 6. (a) DPV studies of Zr(MoO$_4$)$_2$/rGO at different concentration of HQ varying from 0.01 μM to 250 μM (b) linearity plot (c) interference studies plot with closer view inset shown at the top and (d) bar diagram.

Differential pulsed voltammetry studies were done in the presence of 0.1M PB solution with $Zr(MoO_4)_2$/rGO modified glassy carbon electrode for particular property recognition as sensitivity, selectivity repeatability, reproducibility and stability studies.

Table 1. Comparison table for $Zr(MoO_4)_2$/rGO detection of HQ with previously reported papers.

Modified electrode	Linearity (µM)	Technique	Limit of detection (LOD)µM	Reference
GCE/EGr-Au	0.3-100	SWV	0.1	[33]
Graphene/GCE	1-10-10-80	DPV	0.8	[34]
GCE-2	25-2500	SWV	0.61	[35]
P-GCE	0.6-2350	DPV	0.49	[36]
Fe_2O_3/SWCNTs/FTO	1-260	DPV	0.5	[37]
Cu-MOF-199/GCE	0.1-1453	DPV	0.080	[38]
Carbon dots/GCE	0.1-50	DPV	0.1	[39]
$ZrMo_4$/rGO/GCE		DPV	0.020	Present work

Concentration varying from 0.01 µM to 250 µM was added and we could see a linear increased current response as good sensing ability of the modified electrode. Figure 6a depicts the DPV analysis for varying concentrations of HQ ranging from 0.01 to 250 µM under the potential range from -0.4 to 0.6 V in the presence of 0.1M of PB solution and fig.6b its linearity plot. The calculated linear equation was almost y=0.0552x + 0.6972 with correlation coefficient of R^2=0.9933. The LOD value was calculated from the respective DPV plot and obtained value was about 0.020 µM.

3.4. Anti-interference studies

Interference studies was also determined to record whether the $Zr(MoO_4)_2$/rGO modified electrode interferes with the closely relating compounds as like ascorbic acid (AA), glucose (Gu), potassium ions (K^+), sodium ions (Na^+), potassium bromide (KBr), sodium nitride ($NaNO_2$), uric acid (UA). Figure 6c depicts the interference studies performed in DPV with the compounds as described with higher concentrations than HQ and also its clearer view is being shown as an inset. HQ showed very high current response and was selective than the other closely relating compounds with high selectivity and good anti-interference ability. Figure.5d shows the bar diagram for the interference studies. Thus, the as produced $Zr(MoO_4)_2$/rGO modified electrode have the ability of sensing the particular compound HQ with good selectivity.

3.5. Repeatability, reproducibility and stability studies

The repeatability studies were done by repeated experiments with the utilization of $Zr(MoO_4)_2$/rGO modified glassy carbon electrode in the presence of 0.1 M PB solution at the sweep rate

about 0.05 Vs^{-1}. Figure 6a represents the repeatability studies of Zr(MoO$_4$)$_2$/rGO under DPV technique. We could understand its effective concert in a good manner as similar current responses agreed their repeatable studies very well for several repeats. The Zr(MoO$_4$)$_2$/rGO modified GCE was exposed to several independent electrodes for the detection of HQ whereas Figure 7b shows its respective studies performed. The fabricated electrode showed similar response with all the performed electrodes with minor variations exhibiting very good reproducibility of the material. Asides this its stability studies convey a stable response as done for 20 days which is shown in Figure 7c. It was done by keeping the modified electrode in 2°C for 20 days with break for 5 day measurements were done and it exhibits good results with very low error which was due to the unwanted particles present over their surface.

3.6. Real sample analysis

Table 2. Real sample analysis of HQ in tap water, river water and waste water.

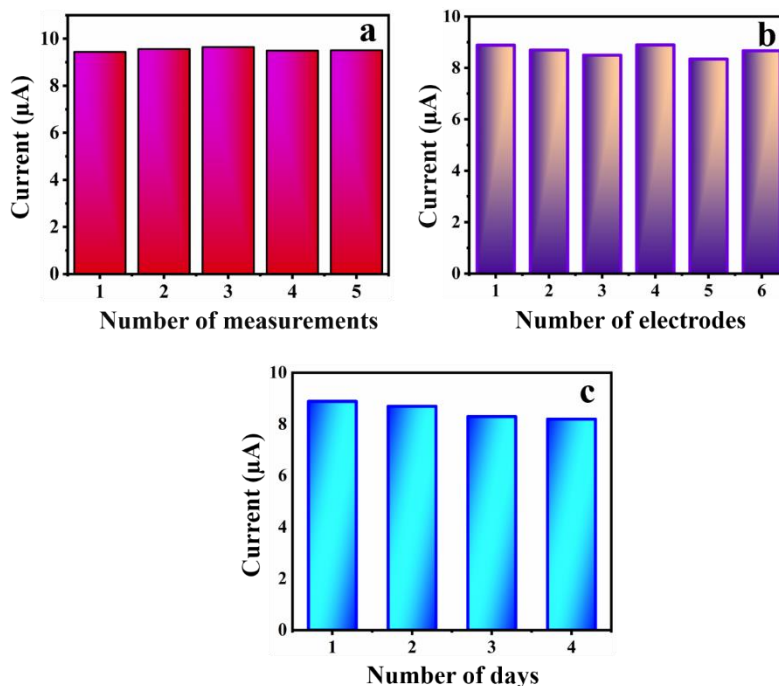| Real Samples	5-ASA		
	Added/μM	Found/μM	Recovery (%)
Tap water	50.0	49.8	99.6
	100.0	98.9	98.9
	150.0	149.7	99.8
River water	50.0	49.5	99
	100.0	99.1	99.1
	150.0	148.8	99.2
Waste water	50.0	47.5	95.1
	100.0	97.9	97.9
	150.0	149.1	99.4.

Figure 7. (a) Repeatability studies of Zr(MoO$_4$)$_2$/rGO **(b)** reproducibility studies and **(c)** stability analysis.
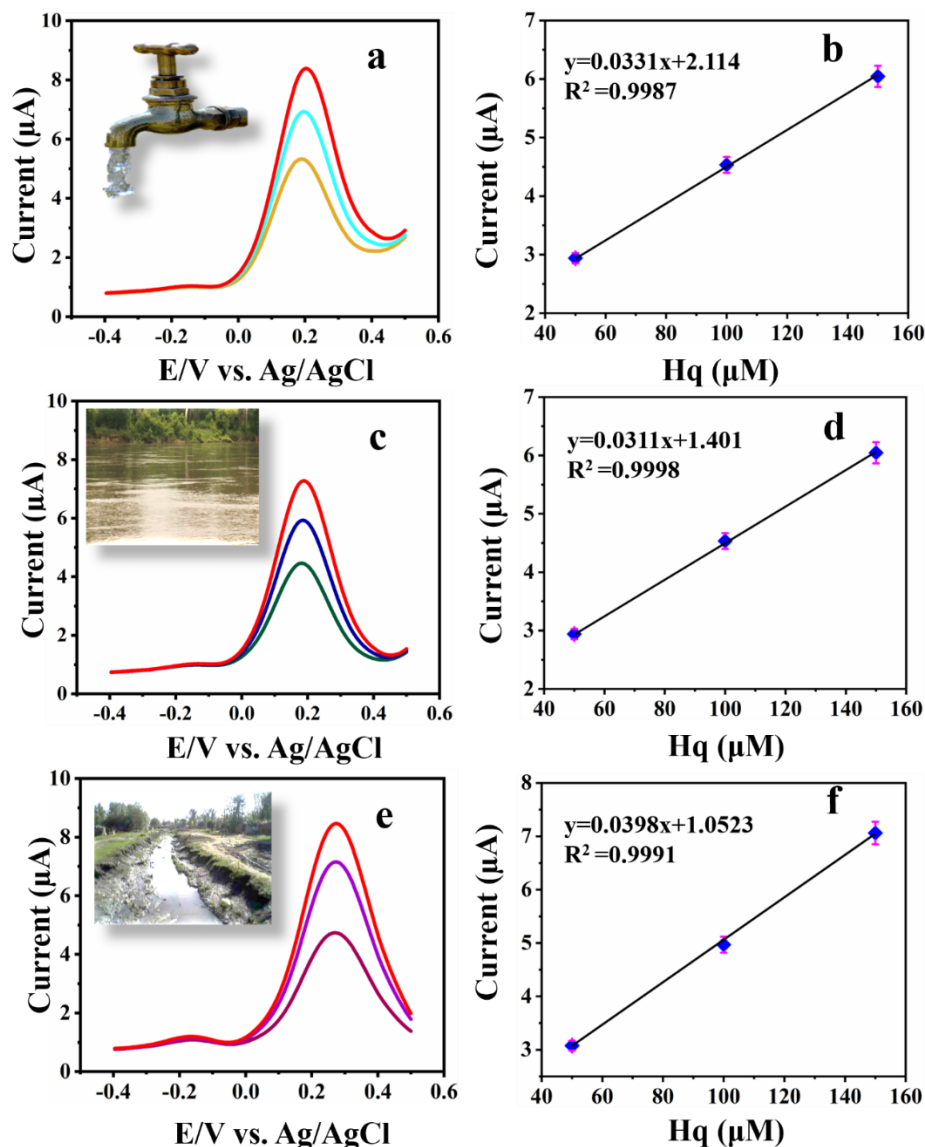
Figure 8. (a) real sample analysis performed with DPV technique for tap water **(b)** river water and **(c)** waste water.

For the practical application of the fabricated electrode real sample analysis has to be done. Herein, Figure 8 a,b,c represents the real sample analysis done with tap water, river water and waste water. Initially, further sensing was carried out by standard addition method in PB solution containing the requires real samples and gradually HQ was spiked over for the sensing. This particular study was done by DPV technique within the potential window -0.4-0.6 V with $Zr(MoO_4)_2$/rGO modified GCE. The gradual increase with the real samples revealed the sensing ability of the sensor opting for real time applications. The regression equation and the respective R^2 values were about y=0.0331x + 2.114, R^2=0.9987, y=0.0311x+1.401, R^2=0.9998. y=0.0398x + 1.0523, R^2=0.9991 for all the three real samples. And with this the obtained recovery values too validated good result which is shown in the table 2.

4. CONCLUSION

In summary, the as synthesized $Zr(MoO_4)_2$/rGO by facile hydrothermal method after characterization revealed their presence with good crystallinity, phase structure, and vibrational property from the XRD analysis and FTIR studies. Further, EIS studies showed very high conductivity of $Zr(MoO_4)_2$ /GCE in comparison with $Zr(MoO_4)_2$ /GCE and rGO/GCE offering the betterment performance of the modified electrode towards HQ detection. The uniform dispersion further accelerates the electrons for enhanced performance of the sensor. As, a result the composite acts well as a mediator of electron transfer for the oxidation of hydroquinone to benzoquinone. Whereas, $Zr(MoO_4)_2$ /GCE was very well significant with 2-electron and two proton transfer as a reversible reaction took place. Moreover, the scrutinized results show the effective sensitivity, selectivity and reproducibility experienced by the sensor is remarkably suitable for the detection of hydroquinone. Along with this the applicability over real samples also establishes satisfactory results with tap water, river water and waste water.

COMPETING INTERESTS
The author(s) declare no competing interests.

References

1. W. Tang, M. Zhang, W. Li, X. Zeng, *Talanta*, 127 (2014) 262–268.
2. A.T.E. Vilian, S.M. Chen, L.H. Huang, M.A. Ali, F.M.A. Al-Hemaid, *Electrochim. Acta*, 125 (2014) 503–509.
3. T. Gan, J. Sun, K. Huang, L. Song, Y. Li, *Sensors Actuators, B Chem.*, 177 (2013) 412–418.
4. M. Lakić, A. Vukadinović, K. Kalcher, A.S. Nikolić, D.M. Stanković, *Talanta*, 161 (2016) 668–674.
5. S. Hu, Y. Wang, X. Wang, L. Xu, J. Xiang, W. Sun, *Sensors Actuators, B Chem.*, 168 (2012) 27–33.
6. L. Yang, H. Zhao, S. Fan, B. Li, C.P. Li, *Anal. Chim. Acta*, 852 (2014) 28–36.
7. R. Sakthivel, R. Sakthivel, M. Annalakshmi, S. Chen, S. Kubendhiran, *J.Electrochemical. Soc.,* 166 (2019) B680-B689.
8. G. Xu, B. Tang, S. Jing, J. Tao, *Int.J.Electrochem.Sci.,* 10 (2015) 10659–10667.
9. A.J.S. Ahammad, T. Akter, A. Al Mamun, T. Islam, M.M. Hasan, M.A. Mamun, S. Faraezi, F.Z. Monira, J.K. Saha, *J. Electrochem. Soc.*, 165 (2018) B390–B397.
10. S. Erogul, S.Z. Bas, M. Ozmen, S. Yildiz, *Electrochim. Acta*, 186 (2015) 302–313.
11. T. Chen, S. Palanisamy, S. Chen, V. Velusamy, T. Tseng, M. Yu, S. Lee, W. Chang, X. Liu, 12 (2017) 8021–8032.
12. Y. Zhang, R. Sun, B. Luo, L. Wang, *Electrochim. Acta*, 156 (2015) 228–234.
13. J. Ahmed, M.M. Rahman, I.A. Siddiquey, A.M. Asiri, M.A. Hasnat, *Sensors Actuators, B Chem.*, 256 (2018) 383–392.
14. Y. Hu, Z. Xue, H. He, R. Ai, X. Liu, X. Lu, *Biosens. Bioelectron.*, 47 (2013) 45–49.
15. M. Rafiq, H. Siddiqui, A.I. Al-wassil, 15 (2012) 986–989.

16. L. Kumari, G.H. Du, W.Z. Li, R.S. Vennila, S.K. Saxena, D.Z. Wang, *Ceram. Int.*, 35 (2009) 2401–2408.
17. C. Lind, D.G. Vanderveer, A.P. Wilkinson, J. Chen, M.T. Vaughan, D.J. Weidner, *Chem.Matter.,* 13 (2001) 487–490.
18. J.M. Hernández Enríquez, L.A. Cortez Lajas, R. García Alamilla, A. Castillo Mares, G. Sandoval Robles, L.A. García Serrano, *J. Alloys Compd.*, 483 (2009) 425–428.
19. H. Teymourian, A. Salimi, S. Firoozi, A. Korani, S. Soltanian, *Electrochim. Acta*, 143 (2014) 196–206.
20. S. Sagadevan, J. Podder, I. Das, *J. Mater. Sci. Mater. Electron.*, 27 (2016) 5622–5627.
21. T. Kokulnathan, T. Chen, S. Chen, J. Vinoth, S. Sakthinathan, E.R. Nagarajan, *Compos. Part B*, 169 (2019) 249–257.
22. Inamuddin, Y.A.Ismail, *Desalination.,* 250 (2010) 523-529.
23. T. Kokulnathan, S. Sakthinathan, S. Chen, *Inorg.Chem.Front.,* 5 (2018) 1145–1155.
24. M.Keerthi, G.Boopathy, S.M.Chen, T.W.Chen, S.P.Rwei, X.Liu, *Int.J.Electrochem.Sci.,* 14 (2019) 346-358.
25. M. Venu, S. Venkateswarlu, Y. Veera, M. Reddy, A.S. Reddy, V.K. Gupta, M. Yoon, G. Madhavi, *ACS.Omega.,* 3 (2018) 14597-14605.
26. S. Radhakrishnan, K. Krishnamoorthy, C. Sekar, J. Wilson, S. Jae, *Chem. Eng. J.*, 259 (2015) 594–602.
27. J. Vinoth Kumar, R. Karthik, S.M. Chen, N. Raja, V. Selvam, V. Muthuraj, *J. Colloid Interface Sci.*, 500 (2017) 44–53.
28. N. Tadros, E. Metwally, *Radiochemistry*, 48 (2006) 387–391.
29. B.S.M. Rao, E. Gantner, J. Reinhardt, D. Steinert, H.J. Ache, *J. Nucl. Mater.*, 170 (1990) 39–49.
30. R.Madhu, S.Palanisamy, S.M. Chen, S, Piraman, *J.electroanalytical chemistry.,*727 (2014) 84-90.
31. S.Sakthinathan, T.Kokulnathan, S.M,Chen, R.Karthik,T.W.Chiu, *Inorg.Chem.Front.,* 5 (2018) 490.
32. A. Umar, A.A. Ibrahim, R. Kumar, T. Almas, P. Sandal, M.S. Al-Assiri, M.H. Mahnashi, B.Z. AlFarhan, S. Baskoutas, *Ceram. Int.*, 46 (2020) 5141–5148.
33. F. Pogacean, M. Coros, L. Magerusan, M.C. Rosu, C. Socaci, S. Gergely, R.I.S. Van Staden, M. Moldovan, C. Sarosi, S. Pruneanu, *Nanotechnology*, 29 (2018).
34. S.J. Li, Y. Xing, G.F. Wang, *Microchim. Acta*, 176 (2012) 163–168.
35. K. Ahmad, P. Kumar, S.M. Mobin, *Nanoscale Adv.*, 2 (2020) 502–511.
36. P. Zhao, M. Ni, C. Chen, C. Wang, P. Yang, X. Wang, C. Li, Y. Xie, J. Fei, *Electroanalysis* , 32 (2020) 1–11.
37. Y. Liu, H. Liao, Y. Zhou, Y. Du, C. Wei, J. Zhao, S. Sun, J.S.C. Loo, Z.J. Xu, *Electrochim. Acta*, 180 (2015) 1059–1067.
38. J. Zhou, X. Li, L. Yang, S. Yan, M. Wang, D. Cheng, Q. Chen, Y. Dong, P. Liu, W. Cai, C. Zhang, *Anal. Chim. Acta*, 899 (2015) 57–65.
39. Z. Li, P. Ni, H. Dai, Z. Li, Y. Sun, J. Hu, S. Jiang, Y. Wang, *Talanta*, 144 (2015) 258–262.